

# CHANDRA AND XMM-NEWTON DISCOVERY OF THE TRANSIENT X-RAY PULSAR IN THE NEARBY SPIRAL GALAXY NGC2403

SERGEY P. TRUDOLYUBOV

Institute of Geophysics and Planetary Physics, University of California, Riverside, CA 92521, and  
 Space Research Institute, Profsoyuznaya 84/32, Moscow, 117997, Russia

WILLIAM C. PRIEDHORSKY

Los Alamos National Laboratory, Los Alamos, NM 87545

AND FRANCE A. CORDOVA

Institute of Geophysics and Planetary Physics, and  
 Department of Physics and Astronomy, University of California, Riverside, CA 92521  
*Draft version May 26, 2019*

## ABSTRACT

We report on the discovery and analysis of the transient X-ray pulsar CXO/XMMU J073709.13+653544 detected in the 2004 August–October *Chandra* and *XMM-Newton* observations of the nearby spiral galaxy NGC2403. The X-ray source exhibits X-ray pulsations with a period  $P \sim 18$  s and a nearly sinusoidal pulse shape and pulsed fraction 46–70% during the first three observations. A detailed timing analysis reveals a rapid decrease of the pulsation period from 18.25 s on Aug. 9 to 17.93 s on Sep. 12 and 17.56 s on Oct. 3, 2004. The X-ray spectra of CXO/XMMU J073709.13+653544 are hard and are well fitted with an absorbed simple power law of photon index  $\Gamma \sim 0.9 - 1.2$  in the 0.3–7 keV energy band. The X-ray properties of the source and the absence of an optical/UV counterpart brighter than 20<sup>th</sup> magnitude allow us to identify CXO/XMMU J073709.13+653544 as accreting X-ray pulsar in NGC2403. The maximum unabsorbed luminosity of the source in the 0.3–7 keV range,  $L_X \sim 2.6 \times 10^{38}$  ergs s<sup>-1</sup> at 3.2 Mpc, is at least 260 times higher than its quiescent luminosity, and exceeds the isotropic Eddington limit for a 1.4M<sub>⊙</sub> compact object. The corresponding estimated luminosity in the 0.3–100 keV energy range could be as high as  $\sim 1.2 \times 10^{39}$  ergs s<sup>-1</sup>, assuming the typical pulsar energy spectrum with high-energy cut-off at 10–20 keV. The rate of decrease of the pulsation period of the source ( $\dot{P} \sim -10^{-7}$  s s<sup>-1</sup>) is the fastest observed among accreting pulsars. The evolution of the pulsation period suggests that it is dominated by the intrinsic spin-up of the compact object, which is almost certainly a neutron star. The accretion rate implied by X-ray luminosity of CXO/XMMU J073709.13+653544 is high enough to account for the observed spin-up rate, assuming that the X-ray source is powered by disk accretion onto highly magnetized neutron star. Based on the transient behavior and overall X-ray properties of the source, we conclude that it could be an X-ray pulsar belonging to either a Be binary system or a low-mass system similar to the transient Galactic bursting pulsar GRO J1744–28.

*Subject headings:* galaxies: individual (NGC2403) — X-rays: binaries — X-rays: stars

## 1. INTRODUCTION

The observations of accretion-powered X-ray pulsars provide a unique opportunity to study the dynamical properties of accreting matter and its interaction with the magnetosphere of a neutron star, and the transfer of the angular momentum in a binary system (White, Swank & Holt 1983; Nagase 1989; Bildsten et al. 1997). Most of the known accreting X-ray pulsars are found in the high-mass binary systems involving a neutron star and OB donor star (either supergiant or Be type) and are associated with younger stellar populations (Corbet 1986; Charles & Coe 2006). These two types correspond to different modes of accretion with supergiant systems accreting from a radially outflowing stellar wind, and the Be binaries accreting from a circumstellar disk. Therefore, the accreting pulsars with supergiant companions are observed as persistent X-ray sources, while the Be systems are recurrent transients and highly variable sources and reach much higher X-ray luminosities up to  $10^{38} \sim 10^{39}$  ergs s<sup>-1</sup>. A small number of X-ray pulsars is associated with low-mass binary systems with mass donors ranging from a main-sequence stars to degenerate carbon-oxygen dwarfs and red giants and can

reach persistent luminosities of  $\gtrsim 10^{38}$  ergs s<sup>-1</sup> (Nagase 1989; Bildsten et al. 1997).

Until recently, the study of X-ray pulsars was limited to our Galaxy and the nearby Magellanic Clouds due to the limited sensitivity and spatial resolution of previous X-ray missions. With the advent of the *Chandra* and *XMM-Newton* X-ray observatories, it has become possible to study the spectral and timing properties of individual X-ray sources associated with more distant galaxies, including bright X-ray pulsators (Fabbiano & White 2006; Fabbiano 2006). For example, recent *XMM-Newton* observations of M31 revealed a 865 s pulsating supersoft X-ray source and a 197 s accreting X-ray pulsar candidate with luminosities of  $\sim 10^{37}$  ergs s<sup>-1</sup> and pulsed fractions of  $\sim 40\%$  (Osborne et al. 2001; Trudolyubov et al. 2005). These results demonstrate that bright pulsating X-ray sources ( $L_X \gtrsim 10^{38}$  ergs s<sup>-1</sup>) can be detected with *XMM-Newton* and *Chandra* in the galaxies beyond the Local Group up to the distances of a few Mpc.

The spiral Scd galaxy NGC2403 at 3.2 Mpc (Freedman & Madore 1988), provides a good opportunity to study X-ray source populations in a normal galaxy. NGC 2403

was a target of previous X-ray observations with the *Einstein* (Fabbiano & Trinchieri 1987; Fabbiano et al. 1992) and *ASCA* observatories (Kotoku et al. 2000), which detected five discrete sources with one bright source classified as an ultraluminous X-ray source (ULX). Recent *Chandra* observations covering the inner  $\sim 25\%$  of the  $D_{25}$  area of NGC2403 have revealed 41 discrete sources with apparent luminosities down to  $\sim 10^{36}$  ergs s $^{-1}$  and allowed to study unresolved soft X-ray emission from the galactic disk (Schlegel & Pannuti 2003; Fraternali et al. 2002).

In this paper, we report on the discovery of the transient pulsating X-ray source CXO/XMMU J073709.13+653544 in NGC2403 using publicly available August-October 2004 observations made with *Chandra* and *XMM-Newton* as a part of the follow-up program studying recent supernova SN 2004dj (Pooley & Lewin 2004; Beswick et al. 2005).

## 2. OBSERVATIONS AND DATA REDUCTION

In our analysis we used the data of three 2004 Aug.-Oct. *Chandra*/ACIS-S observations of SN 2004dj (Table 1). The data of *Chandra* observations was processed using the CIAO v3.3<sup>1</sup> threads. We performed standard screening of the *Chandra* data to exclude time intervals with high background levels, and found no flares exceeding 20% of the average background level. For each observation, we generated X-ray images in the 0.3-7 keV energy band, and used CIAO wavelet detection routine *wavdetect* to detect point sources. Only data in the 0.3-7 keV energy range was used in the spectral analysis of ACIS-S observations. The standard CIAO *xbary* tool was used to produce a barycenter-corrected source event lists used in the timing analysis. To produce source filtered event lists and spectra, we extracted counts within the elliptical region with semi-axes of 2" and 2.5" centered at the position of CXO/XMMU J073709.13+653544. Background counts were extracted from the adjacent source-free regions with subsequent normalization by ratio of detector areas.

We also use the data of 2004 September 12-13 *XMM-Newton* observation of NGC2403 (Table 1) with three European Photon Imaging Camera (EPIC) instruments (MOS1, MOS2 and pn)(Turner et al. 2001; Strueder et al. 2001), and the Optical Monitor (OM) telescope (Mason et al. 2001). We reduced *XMM* data using *XMM-Newton* Science Analysis System (SAS v 6.5.0)<sup>2</sup>. We filtered the original EPIC event files based on the good time intervals produced from the light curves extracted from the whole detector in the 0.2-12 keV energy band by applying an upper count rate threshold of 6 and 2 counts s $^{-1}$  for the EPIC pn and MOS cameras. The last  $\sim 20$  ks of the EPIC observation is affected by high background, and has been excluded from analysis. The standard SAS tool *barycen* was used to perform barycentric correction on the original EPIC event files used for timing analysis.

We generated EPIC-pn and MOS images of NGC2403 field in the 0.3-7.0 keV energy band, and used the SAS standard maximum likelihood (ML) source detection script *edetect\_chain* to detect point sources. We used bright X-ray sources with known counterparts from USNO-B catalog (Monet et al. 2003) and *Chandra* source lists to correct EPIC image astrometry. The astrometric correction was also applied to the OM images, using cross-correlation with USNO-B catalog. After correction, we estimate residual systematic error in the source positions to be of the order 0.5 – 1" for

both EPIC and OM.

To generate EPIC-MOS light curves and spectra, we used a circular region of 18" radius centered at the position of CXO/XMMU J073709.13+653544. Due to the source proximity to the edge of EPIC-pn CCD, the source counts were extracted from the elliptical region with semiaxes of 18" and 13". The adjacent source-free regions were used to extract background spectra. The source and background spectra were then renormalized by ratio of the detector areas. For spectral analysis, we used data in the 0.3 – 10 keV energy band. To synchronize source lightcurves from individual EPIC detectors, we used the identical time filtering criteria based on Mission Relative Time (MRT), following the procedure described in Barnard et al. (2006).

The energy spectra were grouped to contain a minimum of 20 counts per spectral bin in order to allow  $\chi^2$  statistics, and fit to analytic models using the XSPEC v.12<sup>3</sup> fitting package (Arnaud 1996). EPIC-pn, MOS1 and MOS2 data were fitted simultaneously, but with normalizations varying independently. For timing analysis we used standard XANADU/XRONOS v.5<sup>4</sup> tasks.

In the following analysis we assume a distance of 3.2 Mpc for NGC2403 (Freedman & Madore 1988). All parameter errors quoted are 68% ( $1\sigma$ ) confidence limits.

## 3. RESULTS

### 3.1. Source Position

We discovered a new X-ray source CXO J073709.13+653544 in the data of the 2004 August 9 and detected it in the subsequent August 23 and October 3 *Chandra* observations of the NGC2403 field (Table 1). In addition, the analysis of archival 2004 September 12 *XMM-Newton* observation revealed the presence of a bright X-ray source at the position consistent with CXO J073709.13+653544. The source was not detected in the 2004 December 22 *Chandra* observation (observation ID 4630). Combining the data of three *Chandra* observations, we measure the position of CXO/XMMU J073709.13+653544 to be  $\alpha = 07^h37^m09.139^s$ ,  $\delta = +65^\circ35'44.23''$  (J2000 equinox) with an uncertainty of  $\sim 0.5''$  (Fig. 1).

The search for the optical counterparts using the images from the Digitized Sky Survey did not yield any stellar-like object brighter than  $m_B \sim 20$  within the error circle of CXO/XMMU J073709.13+653544. We used the data of 2003 April 30 and 2004 Sept. 12 *XMM-Newton*/OM observations to search for UV counterparts to the source prior and during its X-ray outburst (Fig. 1). We did not detect any stellar counterparts to CXO/XMMU J073709.13+653544 in the OM images down to the limit of  $\sim 20^m$  in the U and OM UVW1 (291 nm) bands.

### 3.2. Long-Term Flux Evolution

The evolution of X-ray luminosity of CXO/XMMU J073709.13+653544 in the 0.3-7 keV energy band based on the data of 2004 *Chandra* and *XMM-Newton* observations is shown in Fig. 2. The first two August 2004 *Chandra* observations show the overall increase of the source X-ray luminosity in the 0.3-7 keV energy band from  $\sim 1.9 \times 10^{38}$  to  $\sim 2.3 \times 10^{38}$  ergs s $^{-1}$ . The subsequent *XMM-Newton* and *Chandra* observations revealed the gradual decrease of the source luminosity to  $\sim 10^{38}$  ergs s $^{-1}$  on Sept. 12, and  $\sim 5 \times 10^{37}$  ergs s $^{-1}$

<sup>1</sup> <http://asc.harvard.edu/ciao/>

<sup>2</sup> See <http://xmm.vilspa.esa.es/user>

<sup>3</sup> <http://heasarc.gsfc.nasa.gov/docs/xanadu/xspec/index.html>

<sup>4</sup> <http://heasarc.gsfc.nasa.gov/docs/xanadu/xronos/xronos.html>

on Oct. 3, 2004. The source was not detected during the 2004 December 22 *Chandra* observation with an upper limit on its 0.3-7 keV luminosity of  $\sim 10^{36}$  ergs s $^{-1}$  ( $2\sigma$ ). The analysis of archival 2001 April 17 *Chandra* observation (observation ID 2014) (Schlegel & Pannuti 2003) and 2003 April 30 and September 11 *XMM-Newton* observations (observation IDs 0150651101 and 0150651201) of NGC2403 taken prior to the 2004 outburst, allow us to estimate the average upper limit ( $2\sigma$ ) on the source quiescent luminosity to be  $\lesssim 10^{36}$  ergs s $^{-1}$  in the 0.3 – 7 keV energy band,  $> 230$  times lower than maximum measured outburst luminosity. It should be noted that due to the sparse sampling the observed lightcurve of the source could be a result of either single long ( $\geq 60$  days) outburst or the superposition of a number of shorter outbursts poorly sampled in time.

### 3.3. X-ray Pulsations

We performed a timing analysis of the CXO/XMMU J073709.13+653544 using the data from *Chandra*/ACIS-S and *XMM-Newton*/EPIC detectors in the 0.3-7 keV energy band. After a barycentric correction of the photon arrival times in the original event lists, we performed a Fast Fourier Transform (FFT) analysis using standard XRONOS task *powspec*, in order to search for coherent periodicities. For the analysis of *XMM-Newton* data, we used combined synchronized EPIC-pn and MOS lightcurves with 2.6 s time bins to improve sensitivity. We found strong peaks in the Fourier spectra of data from the first two *Chandra* observations and *XMM* observation at the frequencies of  $(5.48-5.58) \times 10^{-2}$  Hz (Fig. 3, *left panels*). The strengths of the peaks in the individual Fourier spectra (Fig. 3) correspond to the period detection confidence of  $\sim 10^{-10}$ ,  $\sim 10^{-11}$  and  $\sim 10^{-17}$  for the Aug. 9, 23 *Chandra* and Sept. 12 *XMM-Newton* observations (disregarding simultaneous detection in all three observations).

To estimate the pulsation periods more precisely and determine period errors, we used an epoch folding technique, assuming no period change during individual observations. The most likely values of the pulsation period are listed in Table 2. Then the source lightcurves were folded using the periods determined from epoch folding analysis. The resulting folded lightcurves of CXO/XMMU J073709.13+653544 in the 0.3-7 keV energy band during first three observations are shown in Fig. 3 (*right panels*). The source demonstrates quasi-sinusoidal pulse profiles in the 0.3-7 keV energy band during the first three observations (Fig. 3). The pulsed fraction, defined as  $(I_{\max} - I_{\min}) / (I_{\max} + I_{\min})$ , where  $I_{\max}$  and  $I_{\min}$  represent source intensities at the maximum and minimum of the pulse profile excluding background photons, is significantly higher during the 2004 Aug. 9 *Chandra* observation ( $70 \pm 4\%$ ) when compared to the observations #2 ( $46 \pm 4\%$ ) and #3 ( $56 \pm 3\%$ ) (Table 2).

Although the analysis of the Oct. 3 *Chandra* observation (obs. #4) did not show the presence of a strong single peak in the power density spectrum, we still performed a search for the pulsations in the data of this observation using the epoch folding technique. The epoch folding analysis of the source lightcurve have led to the marginal detection of the pulsation with a period of  $\sim 17.56$  s (Fig. 3, *left panel*). The folded lightcurve of the source in the 0.3-7 keV energy band with a significance of  $\sim 3.7\sigma$  determined using  $\chi^2$  for a nonvarying, constant model, is shown in the upper right panel of Fig. 3. The pulse profile shows a complex non-sinusoidal structure, which probably explains why we do not see strong first harmonic in its Fourier spectrum.

To investigate the energy dependence and time evolution of the source pulse profile, light curves in the soft (0.3-2 keV) and hard (2-7 keV) bands were created for observations #1, 2, and 3<sup>5</sup> and folded at the corresponding best pulsation periods (Figure 4). The corresponding pulsed fractions in the soft and hard energy bands are given in Table 2. As can be seen from Fig. 4 and Table 2, the energy dependence of the pulse profile in the Aug. 9 *Chandra* observation (obs. #1) is qualitatively different from subsequent *Chandra* and *XMM-Newton* observations (obs. #2 and 3). The source modulation amplitude in the soft band is higher than in the hard band during Aug. 9 *Chandra* observation, while the modulation is stronger in the hard band during the Aug. 23 *Chandra* and Sept. 12 *XMM-Newton* observations. The modulation fraction in the soft band is highest (78%) during the Aug. 9 observation, and drops to  $\sim 43\%$  and  $\sim 50\%$  on Aug. 23 and Sept. 12. At the same time, the modulation fraction in the hard energy band remains compatible during all three observations (Table 2; Fig. 4).

### 3.4. Long-term Period Evolution

There is a significant change of the pulsation period of CXO/XMMU J073709.13+653544 measured over the course of four observations covering a  $\sim 55$ -day period from  $P=18.25$  s on Aug. 9, 2004 to  $P=17.56$  s on Oct. 3, 2004 (Table 2; Fig. 5). During the first three observations corresponding to a 35-day time interval, the source shows a roughly linear decrease of the pulsation period. Using these three period measurements and assuming its linear time dependence, we estimate the rate of period change  $\dot{P} \sim -(1.1 \pm 0.2) \times 10^{-7}$  s s $^{-1}$  (pulse frequency derivative  $\dot{\nu} \sim 3.4 \times 10^{-10}$  Hz s $^{-1}$ ), that corresponds to  $(\dot{P}/P) \sim -6 \times 10^{-9}$  s $^{-1} \sim -0.19$  yr $^{-1}$  for a period  $P = 18$  s.

### 3.5. X-ray Spectra

The pulse phase averaged *Chandra*/ACIS-S and *XMM-Newton*/EPIC spectra of CXO/XMMU J073709.13+653544 can be adequately fit with the absorbed simple power law models with photon index,  $\Gamma \sim 0.9 - 1.2$  and an equivalent hydrogen density  $N_H \sim (15 - 58) \times 10^{20}$  cm $^{-2}$ . The corresponding absorbed luminosity of the source in the 0.3-7 keV band ranges between  $\sim 5 \times 10^{37}$  and  $\sim 2.3 \times 10^{38}$  ergs s $^{-1}$ , assuming the distance of 3.2 Mpc. The best-fit spectral model parameters for individual observations are given in Table 2. The luminosity and energy spectra of the source are similar to that of the bright X-ray pulsars in our Galaxy and the Magellanic Clouds (Nagase 1989; Yokogawa et al. 2003). The shape of the energy spectra of CXO/XMMU J073709.13+653544 in the 0.3-7 keV energy band remains essentially constant through the outburst despite significant change of the source luminosity. For all observations, the measured absorbing column  $N_H$  is  $\sim 3$ -10 times higher than the Galactic hydrogen column in the direction of NGC2403,  $4 \times 10^{20}$  cm $^{-2}$  (Dickey & Lockman 1990), consistent with an additional intrinsic absorption within the system and inside the disk of NGC2403.

## 4. DISCUSSION

A combination of transient behavior and the extremely large spin-up rate of CXO/XMMU J073709.13+653544 makes it a unique object among pulsating X-ray sources.

<sup>5</sup> The limited source count statistics in the Oct. 3 observation does not permit a detailed study of energy dependence of pulsations.

The overall X-ray properties (X-ray spectrum, pulsation period etc.) of the source are consistent with that of the accreting X-ray pulsar in a binary system (White, Swank & Holt 1983; Nagase 1989). The absence of bright optical counterparts (both during quiescence and outburst), transient behavior, overall X-ray properties of CXO/XMMU J073709.13+653544 and positional coincidence with NGC2403, allow us to conclude that is almost certainly located outside our Galaxy and belongs to NGC2403. Placing CXO/XMMU J073709.13+653544 at the distance of NGC2403 (3.2 Mpc) implies very high luminosities of the source during the outburst ( $(0.6 \sim 2.4) \times 10^{38}$  ergs s<sup>-1</sup> in the 0.3-7 keV energy band and  $(0.8 \sim 3.8) \times 10^{38}$  ergs s<sup>-1</sup> in the 0.3-10 keV energy band) with maximum observed luminosity exceeding the isotropic Eddington luminosity limit for a  $1.4M_{\odot}$  object. If CXO/XMMU J073709.13+653544 is indeed an accreting X-ray pulsar in NGC2403, the relative rate of change of its pulsation period,  $(\dot{P}/P) \sim -6 \times 10^{-9}$  s<sup>-1</sup> is the highest observed in this class of objects to date (Nagase 1989; Bildsten et al. 1997).

If the X-ray pulsations observed in CXO/XMMU J073709.13+653544 result from rotation of a highly magnetized accreting compact object in a binary system, the change of its pulsation period can be explained by combination of binary orbital motion of the pulsar (Skinner et al. 1982) and transfer of angular momentum in the accretion process (Rappaport & Joss 1977; Ghosh & Lamb 1979). The relatively long time scale on which we observe the decrease of the pulsation period and its high, nearly constant rate suggest that the intrinsic spin-up of the pulsar should make the major contribution to the observed change of the pulsation period. Using the observed pulsation parameters of CXO/XMMU J073709.13+653544, and assuming that disk accretion is occurring in the system, one can make a simple estimate of the lower limit on the accretion rate required to explain the observed spin-up rate  $\dot{P}$ . Let us assume that all the specific angular momentum of the accreting material is transferred to the compact object at the magnetospheric radius  $r_m$ . In order to keep the “propeller” effect from preventing accretion onto compact object, the magnetospheric radius must be less than the corotation radius  $r_m \lesssim r_c = (GM_X/4\pi^2)^{1/3} P^{2/3}$ , where  $P$  is the rotational period and  $M_X$  is a compact object mass (Illarionov & Sunyaev 1975). The maximum torque experienced by compact object  $N = \dot{M}(GM_X r_c)^{1/2}$ , where  $\dot{M}$  denotes the accretion rate through the disk, should be greater or equal to the observed torque  $N_{obs} = I\dot{\omega} = 2\pi I(\dot{P}/P^2)$ , where  $I$  is the moment of inertia of the compact object. As a result, we obtain

$$\dot{M} \gtrsim I(4\pi^2/GM_X)^{2/3} \dot{P} P^{-7/3} \quad (1)$$

or,

$$\dot{M} \gtrsim 5.2 \times 10^{18} f \left( \frac{-\dot{P}}{10^{-7} \text{ s s}^{-1}} \right) \left( \frac{P}{18 \text{ s}} \right)^{-7/3} \text{ g s}^{-1}, \quad (2)$$

where  $f = (I/10^{45} \text{ g cm}^2)(M_X/M_{\odot})^{-2/3}$ . Substituting typical white dwarf parameters ( $I \sim 10^{50} \text{ g cm}^2$ ,  $M_X = M_{\odot}$ ) and the observed rotation period and its derivative into equation (2) gives an unreasonably high mass accretion rate  $\dot{M} \gtrsim 5 \times 10^{23} \text{ g s}^{-1}$ . On the other hand, for a typical neutron star parameters ( $I \sim 10^{45} \text{ g cm}^2$ ,  $M_X = 1.4M_{\odot}$ ) the estimated mass accretion rate required to produce the observed spin-up is  $\dot{M} \gtrsim 4 \times 10^{18} \text{ g s}^{-1} = 6.3 \times 10^{-8} M_{\odot} \text{ year}^{-1}$ . The corresponding bolometric luminosity of the  $1.4M_{\odot}$  neutron star accreting at such rate should be  $L_{bol} \gtrsim 7.3 \times 10^{38} \text{ ergs s}^{-1}$ , assuming that all gravitational energy of the infalling matter released in the process

of accretion is converted into radiation. The estimated bolometric luminosity of the source is very high, exceeding the Eddington critical luminosity for a  $1.4M_{\odot}$  star at least by factor of 4.

It is interesting to compare the luminosity required from accretion spin-up mechanism to the total X-ray luminosity of the source during the outburst. In order to estimate the total X-ray luminosity of CXO/XMMU J073709.13+653544, we extrapolated the results of our spectral analysis to the higher energies, assuming that the broad-band spectrum of the source in the 0.3-100 keV band is represented by a power law with high-energy cutoff at energies above 10-20 keV, as typically observed in the accreting X-ray pulsars (White, Swank & Holt 1983; Nagase 1989). To model the broad-band spectrum, we used a simple power law model with photon index and normalization derived from spectral fitting in the 0.3-7 keV band, modified at energies above a high-energy cutoff  $E_c$  by the function  $\exp[(E_c - E)/E_f]$ , where  $E_f$  is the folding energy. For the Aug. 23 observation, the estimated X-ray luminosity of CXO/XMMU J073709.13+653544 in the 0.3-100 keV energy band falls between  $\sim 8 \times 10^{38}$  and  $1.2 \times 10^{39} \text{ ergs s}^{-1}$  for  $E_c = 10 \sim 20 \text{ keV}$  and  $E_f = 10 \text{ keV}$ . Note that this estimate should be regarded as a lower limit, as it does not account for the possible presence of the soft ( $kT \sim 0.1-0.2 \text{ keV}$ ) component in the spectrum of the source, similar to that observed in some of the bright X-ray pulsars (Yokogawa et al. 2003). Therefore, the estimated maximum X-ray luminosity of CXO/XMMU J073709.13+653544 is high enough to account for the observed spin-up rate, assuming that the X-ray source is powered by disk accretion onto highly magnetized neutron star.

The estimated maximum luminosity of the source can be used to put an upper limit on the strength  $B_0$  of the magnetic field of the neutron star. Assuming the dipole configuration of the pulsar magnetic field, and requiring the magnetospheric radius to be smaller than corotation radius  $r_m \lesssim r_c$ , we obtain

$$B_0 \lesssim 7 \times 10^{13} f_1 \left( \frac{P}{18 \text{ s}} \right)^{7/6} \left( \frac{L_X}{10^{39} \text{ ergs s}^{-1}} \right)^{1/2} \text{ G} \quad (3)$$

where  $f_1 = (R/10^6 \text{ cm})^{-5/2} (M_X/M_{\odot})^{1/3}$  and  $R$  is the radius of the neutron star.

Although both the observed luminosity of the source and luminosities required by spin-up due to disk accretion are extremely high, they lie within the range observed for pulsating neutron stars that can reach luminosities of  $\sim 5 - 10 \times 10^{38} \text{ ergs s}^{-1}$  (White & Carpenter 1978; Skinner et al. 1982; Nagase 1989). The required luminosities are also consistent with theoretical predictions for super-Eddington accretion onto highly magnetized ( $B \gtrsim 10^{12} \text{ G}$ ) neutron star (Basko & Sunyaev 1976). At high accretion rates, the accreting matter is expected to release its gravitational energy inside accretion columns above the magnetic poles of the neutron star. Since most of radiation is emitted from the sides of these columns, it can escape the system without crossing the bulk of the inflowing accreting matter. This anisotropy allows the luminosity of the neutron star to exceed formal Eddington limit by large factors. For the accretion column with a cross-section in the form of a thin ring segment of length  $l$  and thickness  $d$ , the limiting luminosity that can be reached in the Basko & Sunyaev (1976) model is given by

$$L_{max} \sim 8 \times 10^{38} \left( \frac{l/d}{40} \right) \left( \frac{M_X}{M_{\odot}} \right) \text{ ergs s}^{-1} \quad (4)$$

Therefore, for the highly super-Eddington accretion rate and  $l \gg d$  the emission from accretion columns could explain the observed high luminosity of CXO/XMMU J073709.13+653544.

The measured pulse period places CXO/XMMU J073709.13+653544 among Be systems or short-period binary supergiant systems with Roche lobe overflow on a Corbet diagram (pulse period-orbital period plot) (Corbet 1986; Waters & van Kerkwijk 1989; Bildsten et al. 1997). The transient behavior of the source suggests a higher probability for it to be a member of Be binary class, since majority of Be systems display recurrent/transient outbursts. The high peak luminosity of CXO/XMMU J073709.13+653544 ( $L_X \sim 10^{39}$  ergs s $^{-1}$ ) is also not unusual for the Be X-ray pulsars with transient Be X-ray pulsar A0538-66 reaching similar luminosities during its giant outbursts (Skinner et al. 1982).

Using the Corbet diagram, one can try to predict the value of the binary period of CXO/XMMU J073709.13+653544. If it is indeed a Be system, the estimated orbital period  $P_{orb}$  can vary between  $\sim 20$  and  $\sim 100$  days. The observed duration of the source outburst allows us to put further constraints on the value of the binary period. Assuming that we observed a single outburst from the source and that it corresponds to one orbital cycle, we obtain  $60 \lesssim P_{orb} \lesssim 100$  days. Note, however, that if the source went through the giant (class II) outburst lasting for several orbits (Stella, White & Rosner 1986) or a sequence of shorter outbursts during August-October 2004, the orbital period of the system could be much shorter than 60 days.

Another possibility is that CXO/XMMU J073709.13+653544 is a transient low-mass binary sys-

tem. The transient behavior and high luminosity of the source are somewhat similar to that of the Galactic bursting X-ray pulsar GRO J1744-28 (Kouveliotou et al. 1996), that reached a luminosity of  $\sim 10^{39}$  ergs s $^{-1}$  during the peak of its outburst (Giles et al. 1996; Sazonov, Sunyaev & Lund 1997). In the low-mass system scenario, the transient outbursts of the source could be explained by sudden increase of accretion from the disk reservoir (Sunyaev & Shakura 1977) or as a result of the viscous-thermal instability of the quiescent accretion disk.

The discovery of X-ray pulsations in CXO/XMMU J073709.13+653544 is yet another demonstration that deep monitoring observations with *Chandra* and *XMM-Newton* have a great potential in revealing populations of both persistent and transient pulsating X-ray sources in nearby galaxies. Future observations of CXO/XMMU J073709.13+653544, if it reappears, could possibly give deeper insight into the behavior of this and other similar X-ray pulsar systems. The complete coverage of the source outbursts with more frequent sampling would allow to estimate the orbital parameters of the system and help to determine its nature.

## 5. ACKNOWLEDGMENTS

Support for this work was provided through NASA Grant NAG5-12390. This research has made use of data obtained through the High Energy Astrophysics Science Archive Research Center Online Service, provided by the NASA/Goddard Space Flight Center. XMM-Newton is an ESA Science Mission with instruments and contributions directly funded by ESA Member states and the USA (NASA).

## REFERENCES

- Arnaud, K. 1996, in *Astronomical Data Analysis Software and Systems V*, ASP Conference Series 101, ed. G. Jacoby & J. Barnes (San Francisco: ASP) 17
- Beswick, R. J., Muxlow, T. W. B., Argo, M. K., Pedlar, A., Marcaide, J. M., & Wills, K. A. 2005, *ApJ*, 623, L21
- Barnard, R., Trudolyubov, S., Kolb, U. C., Haswell, C. A., Osborne, J. P., & Priedhorsky, W. C. 2006, *A&A*, submitted (astro-ph/0610035)
- Basko, M. M., & Sunyaev, R. A. 1976, *MNRAS*, 175, 395
- Bildsten, L., Chakrabarty, D., Chiu, J., Finger, M. H., Koh, D. T., Nelson, R. W., Prince, T. A., Rubin, B. C., Scott, D. M., Stollberg, M., Vaughan, B., Wilson, C. A., & Wilson, R. B. 1997, *ApJSS*, 113, 367
- Charles, P. A., & Coe, M. J. 2006, in *Compact Stellar X-ray Sources*, ed. W. H. G. Lewin & M. van der Klis (Cambridge: Cambridge Univ. Press)
- Corbet, R. H. D. 1986, *MNRAS*, 220, 1047
- Dickey, J. M., & Lockman, F. J. 1990, *ARA&A*, 28, 215
- Fabbiano, G., Kim, D.-W., & Trinchieri, G. 1992, *ApJS*, 80, 531
- Fabbiano, G., & Trinchieri, G. 1987, *ApJ*, 315, 46
- Fabbiano, G., & White, N. E. 2006, in *Compact Stellar X-ray Sources*, ed. W. H. G. Lewin & M. van der Klis (Cambridge: Cambridge Univ. Press)
- Fabbiano, G. 2006, *ARA&A*, 44, 323
- Fraternali, F., Cappi, M., Sancisi, R., & Oosterloo, T. 2002, *ApJ*, 578, 109
- Freedman, W. L., & Madore, B. F. 1988, *ApJ*, 332, L63
- Ghosh, P., & Lamb, F. K. 1979, *ApJ*, 234, 296
- Giles, A. B., Swank, J. H., Jahoda, K., Zhang, W., Strohmayer, T., Stark, M. J., & Morgan, E. H. 1996, *ApJ*, 469, L25
- Illarionov, A. F., & Sunyaev, R. A. 1975, *A&A*, 39, 185
- Kotoku, J., Mizuno, T., Kubota, A., & Makishima, K. 2000, *PASJ*, 52, 1081
- Kouveliotou, C., van Paradijs, J., Fishman, G. J., Briggs, M. S., Komers, J., Harmon, B. A., Meegan, C. A., & Lewin, W. G. H. 1996, *Nature*, 379, 799
- Mason, K. O., Breeveld, A., Much, R., Carter, M., Córdova, F. A., Cropper, M. S., Fordham, J., Huckle, H., Ho, C., Kawakami, H., Kennea, J., Kennedy, T., Mittaz, J., Pandel, D., Priedhorsky, W. C., Sasseeen, T., Shirey, R., Smith, P., & Vreux, J.-M. 2001, *A&A*, 365, 36
- Monet, D. G., et al. 2003, *AJ*, 125, 984
- Nagase, F. 1989, *PASJ*, 41, 1
- Osborne, J. P., Borozdin, K. N., Trudolyubov, S. P., Priedhorsky, W. C., Soria, R., Shirey, R., Hayter, C., La Palombara, N., Mason, K., Molendi, S., Paerels, F., Pietsch, W., Read, A. M., Tiengo, A., Watson, M. G., & West, R. G. 2001, *A&A*, 378, 800
- Pooley, G., & Lewin, W. H. G. 2004, *IAU Circ.* 8390
- Rappaport, S., & Joss, P. C. 1977, *Nature*, 266, 683
- Sazonov, S. Y., Sunyaev, R. A., & Lund, N. 1997, *Astron. Lett.*, 23, 286
- Schlegel, E. M., & Pannuti, T. J. 2003, *AJ*, 125, 3025
- Skinner, G. K., Bedford, D. K., Elsner, R. F., Leahy, D., Weisskopf, M. C., & Grindlay, J. 1982, *Nature*, 297, 568
- Stella, L., White, N. E., & Rosner, R. 1986, *ApJ*, 308, 669
- Strueder, L. et al. 2001, *A&A*, L18
- Sunyaev, R. A., & Shakura, N. I. 1977, *Sov. Astron. Lett.*, 3, 138
- Trudolyubov, S., Kotov, O., Priedhorsky, W., Cordova, F., & Mason, K. 2005, *ApJ*, 634, 314
- Turner, M. et al. 2001, *A&A*, 365, L27
- Waters, L. B. F. M., & van Kerkwijk, M. H. 1989, *A&A*, 223, 196
- White, N. E., & Carpenter, G. F. 1978, *MNRAS*, 183, 11
- White, N. E., Swank, J. H., & Holt, S. S. 1983, *ApJ*, 270, 711
- Yokogawa, J., Imanishi, K., Tsujimoto, M., Koyama, K., & Nishiuchi, M. 2003, *PASJ*, 55, 161

TABLE 1  
*Chandra* AND *XMM-Newton* OBSERVATIONS OF NGC2403 USED IN THE ANALYSIS.

| Obs.# | Date, UT     | Date, TJD        | Obs. ID    | Mission/Instrument      | RA (J2000) <sup>a</sup><br>(h:m:s) | Dec (J2000) <sup>a</sup><br>(d:m:s) | Exp. <sup>b</sup><br>(ks) |
|-------|--------------|------------------|------------|-------------------------|------------------------------------|-------------------------------------|---------------------------|
| 1     | 2004 Aug. 09 | 13226.561(0.273) | 4627       | <i>Chandra</i> /ACIS-S  | 07:37:22.34                        | +65:36:10.7                         | 40.0                      |
| 2     | 2004 Aug. 23 | 13240.701(0.290) | 4628       | <i>Chandra</i> /ACIS-S  | 07:37:21.72                        | +65:36:10.9                         | 46.5                      |
| 3     | 2004 Sep. 12 | 13261.182(0.449) | 0164560901 | <i>XMM-Newton</i> /EPIC | 07:37:17.00                        | +65:35:57.8                         | 59.0(MOS)/52.4(pn)        |
| 4     | 2004 Oct. 03 | 13281.951(0.276) | 4629       | <i>Chandra</i> /ACIS-S  | 07:37:19.45                        | +65:36:29.8                         | 44.5                      |

<sup>a</sup> – pointing coordinates

<sup>b</sup> – instrument exposure used in the analysis

TABLE 2  
X-RAY PULSATION PARAMETERS AND POWER LAW SPECTRAL FIT INFORMATION FOR CXO/XMMU J073709.13+653544.

| Obs. | Period<br>(s)      | PF <sub>0.3–7keV</sub><br>(%) <sup>a</sup> | PF <sub>0.3–2keV</sub><br>(%) <sup>a</sup> | PF <sub>2–7keV</sub><br>(%) <sup>a</sup> | N <sub>H</sub><br>( $\times 10^{20} \text{ cm}^{-2}$ ) | Photon<br>Index                        | Flux <sup>b</sup> | Flux <sup>c</sup> | $\chi^2$<br>(d.o.f) | $L_X^d$ | $L_X^e$ | Instrument  |
|------|--------------------|--|--|--|--|--|-------------------|-------------------|---------------------|---------|---------|-------------|
| 1    | 18.253 $\pm$ 0.003 | 70 $\pm$ 4                                 | 78 $\pm$ 5                                 | 63 $\pm$ 6                               | 37 <sup>+8</sup> <sub>-7</sub>                         | 1.18 <sup>+0.13</sup> <sub>-0.12</sub> | 1.58 $\pm$ 0.07   | 1.96 $\pm$ 0.12   | 25.6(25)            | 1.94    | 2.40    | ACIS-S      |
| 2    | 18.098 $\pm$ 0.003 | 46 $\pm$ 4                                 | 43 $\pm$ 6                                 | 56 $\pm$ 5                               | 20 $\pm$ 5   | 0.96 $\pm$ 0.10                        | 1.90 $\pm$ 0.07   | 2.12 $\pm$ 0.14   | 27.7(33)            | 2.33    | 2.60    | ACIS-S      |
| 3    | 17.934 $\pm$ 0.002 | 51 $\pm$ 3                                 | 50 $\pm$ 6                                 | 64 $\pm$ 4                               | 15 <sup>+5</sup> <sub>-4</sub>                         | 0.88 $\pm$ 0.08                        | 0.89 $\pm$ 0.04   | 0.99 $\pm$ 0.06   | 52.4(64)            | 1.09    | 1.21    | EPIC/pn+MOS |
| 4    | 17.562 $\pm$ 0.006 | ...  | ...  | ...                                      | 58 <sup>+28</sup> <sub>-23</sub>                       | 1.21 <sup>+0.37</sup> <sub>-0.34</sub> | 0.38 $\pm$ 0.03   | 0.50 $\pm$ 0.06   | 3.0(4)              | 0.47    | 0.61    | ACIS-S      |

<sup>a</sup> – pulsed fraction in the 0.3 – 7, 0.3 – 2 and 2 – 7 keV energy bands, defined as  $(I_{\max} - I_{\min}) / (I_{\max} + I_{\min})$ , where  $I_{\max}$  and  $I_{\min}$  represent source background-corrected intensities at the maximum and minimum of the pulse profile

<sup>b</sup> – absorbed model flux in the 0.3 – 7 keV energy range in units of  $10^{-13} \text{ erg s}^{-1} \text{ cm}^{-2}$

<sup>c</sup> – unabsorbed model flux in the 0.3 – 7 keV energy range in units of  $10^{-13} \text{ erg s}^{-1} \text{ cm}^{-2}$

<sup>d</sup> – absorbed luminosity in the 0.3 – 7 keV energy range in units of  $10^{38} \text{ erg s}^{-1}$ , assuming the distance of 3.2 Mpc

<sup>e</sup> – unabsorbed luminosity in the 0.3 – 7 keV energy range in units of  $10^{38} \text{ erg s}^{-1}$ , assuming the distance of 3.2 Mpc

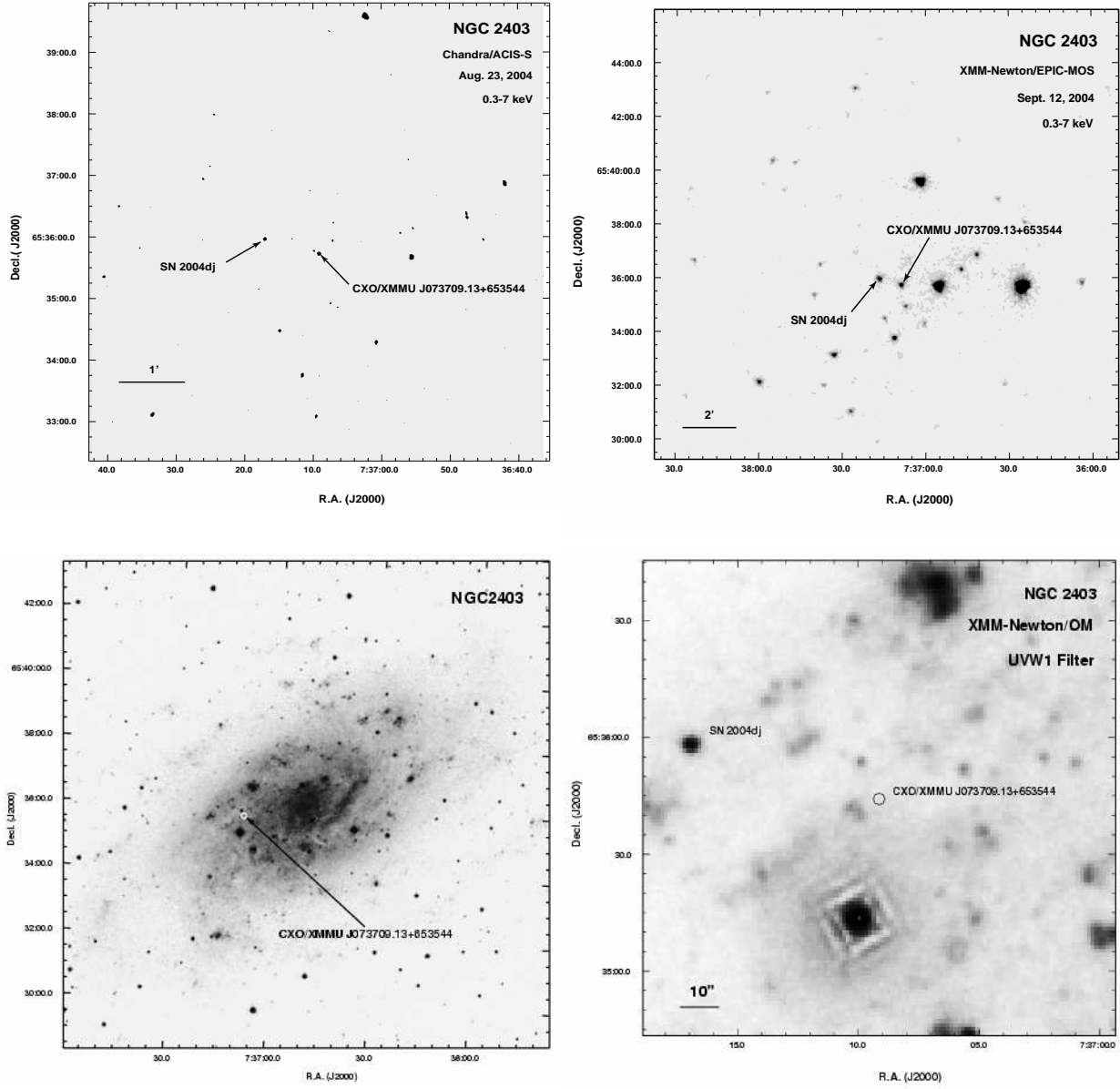


FIG. 1.— *Upper left:* Chandra/ACIS image of NGC 2403 field taken on Aug. 23, 2004. *Upper right:* Combined 0.3-7 keV XMM/EPIC-MOS image of NGC 2403 field taken on Sept. 12, 2004. The positions of a new transient pulsar CXO/XMMU J073709.13+653544 and supernova SN 2004dj are marked with arrows. *Lower left:* Optical B-band image of NGC2403 from the second generation Digitized Sky Survey. The position of CXO/XMMU J073709.13+653544 is shown with white circle. *Lower right:* XMM-Newton/OM UVW1 band image of NGC2403 field taken on Sept. 12, 2004. The position of CXO/XMMU J073709.13+653544 is shown with black circle of 1.5'' radius ( $3\sigma$ ).



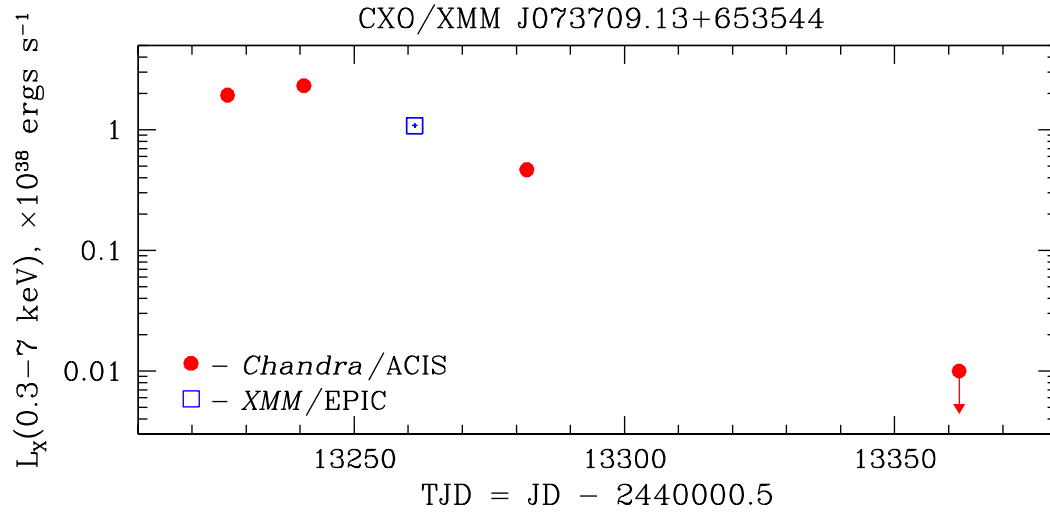


FIG. 2.— The X-ray light curve of CXO/XMMU J073709.13+653544 in the 0.3-7 keV energy band. The luminosities were calculated assuming a source distance of 3.2 Mpc.

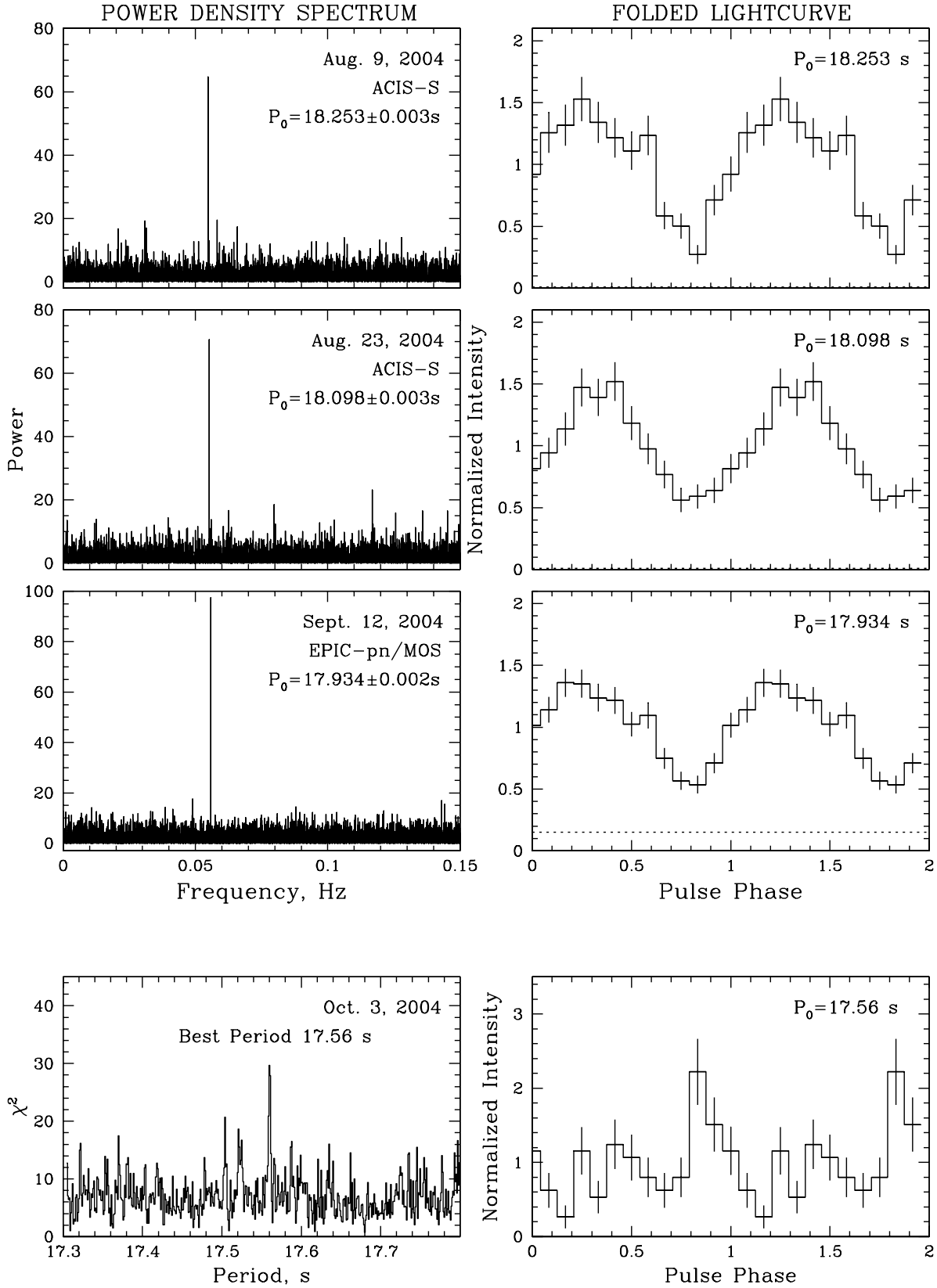


FIG. 3.— (Left upper three panels) Power spectra of CXO/XMMU J073709.13+653544 obtained using the data of 2004 Aug. 9 (upper panel) and Aug. 24 (middle panel) *Chandra*/ACIS-S observations and 2004 Sept. 12 *XMM-Newton*/EPIC observations (lower panel) in the 0.3–7 keV energy band. (Right upper three panels) Corresponding pulse profiles folded with most likely pulsation periods. The background levels are represented by the dotted lines. The ephemeris is defined arbitrarily such as the dip in the pulse profile falls at phase 0.8. (Lower panels) The results of epoch-folding analysis of the data of 2004 Oct. 3 *Chandra*/ACIS observation of the source.

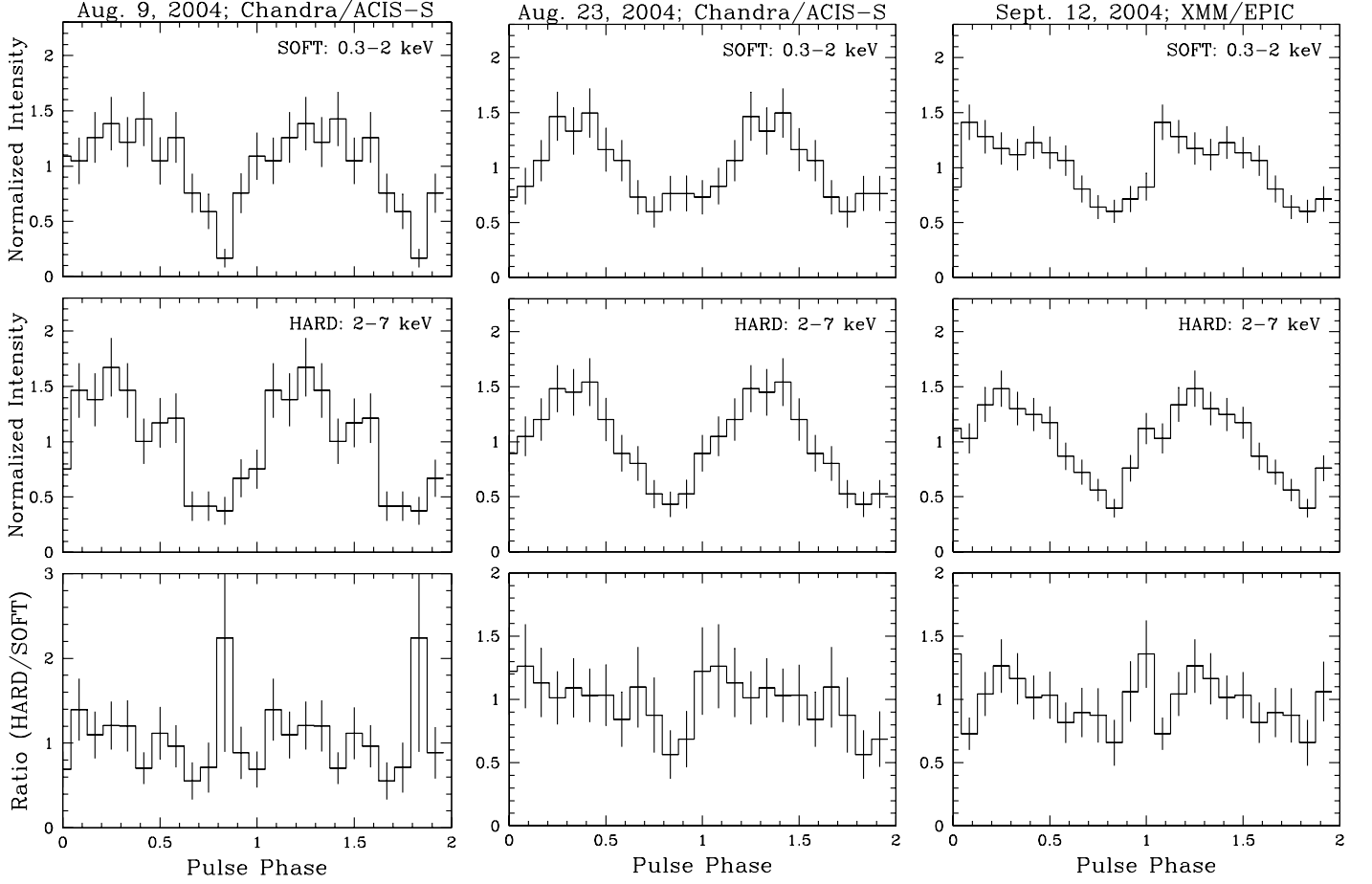


FIG. 4.— X-ray lightcurves of CXO/XMMU J073709.13+653544 during the 2004 Aug. 9 and 23 *Chandra* and Sept. 12 *XMM-Newton* observations folded at the corresponding best periods (Table 2) in the soft (0.3-2 keV) and hard (2-7 keV) energy bands (*upper middle panels*) along with hardness ratios (*bottom panels*).

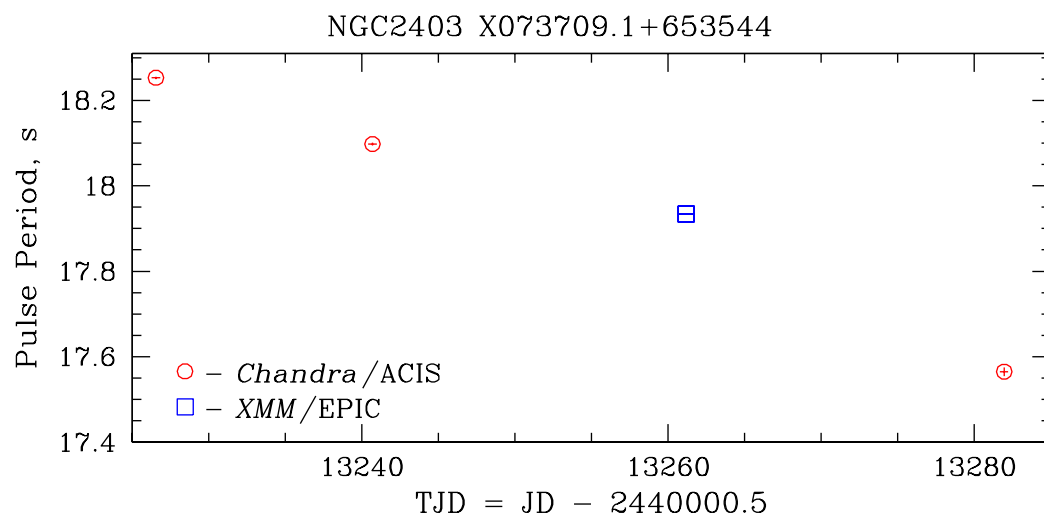


FIG. 5.— The long-term evolution of the pulsation period of CXO/XMMU J073709.13+653544. No orbital corrections have been applied to the pulse frequencies, since the orbital parameters are unknown.

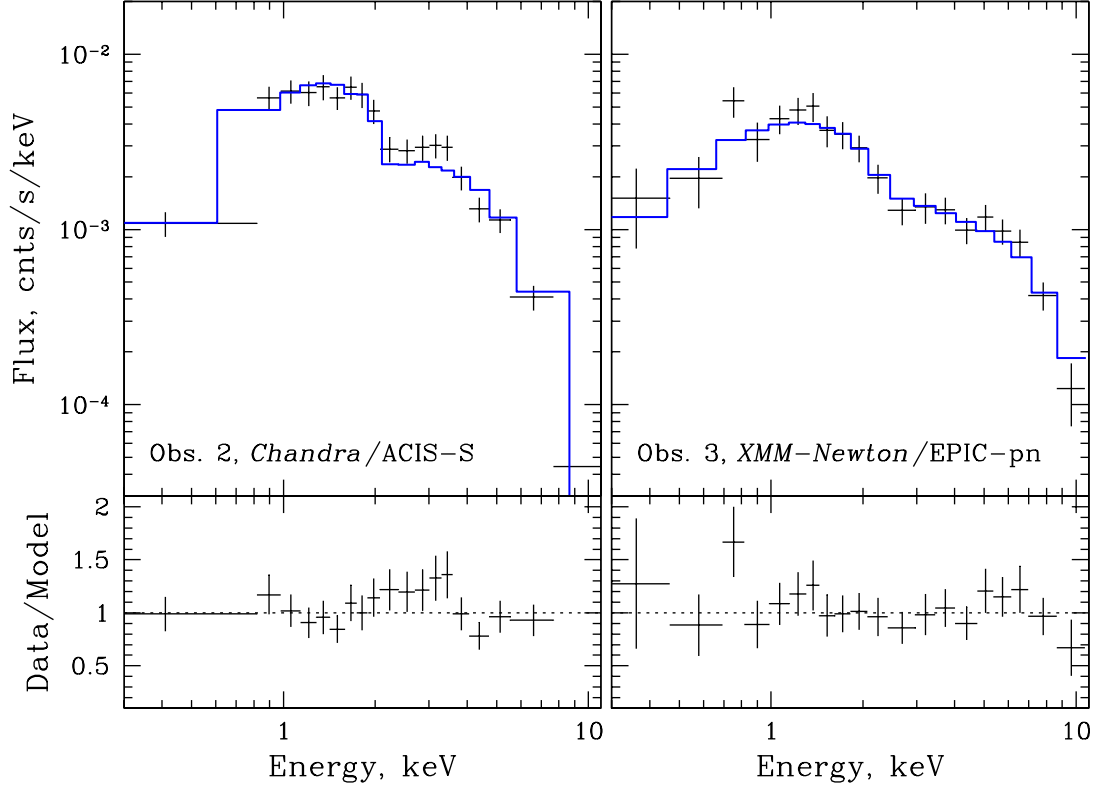


FIG. 6.— (Left panels) Count spectra and model ratios of CXO/XMMU J073709.13+653544 obtained during August 23 *Chandra*/ACIS-S observation of CXO/XMMU J073709.13+653544. (Right panels) EPIC count spectra and model ratios of the source during September 12 *XMM-Newton* observation. The best-fit absorbed power law model approximation is shown with thick histograms.